Impact of Lipid Raft Integrity on 5-HT$_3$ Receptor Function and its Modulation by Antidepressants

Caroline Nothdurfter[1,2,4], Sascha Tanasic[2,4], Barbara Di Benedetto[1,2], Gerhard Rammes[2,3], Eva-Maria Wagner[2], Thomas Kirmeier[2], Vanessa Ganal[2], Julia S Kessler[1,2], Theo Rein[2], Florian Holsboer[2] and Rainer Rupprecht*[1,2]

[1]Department of Psychiatry and Psychotherapy, Ludwig-Maximilians-University Munich, Munich, Germany; [2]Max-Planck-Institute of Psychiatry, Munich, Germany; [3]Department of Anesthesiology, Technische Universität, Munich, Germany

Because of the biochemical colocalization of the 5-HT$_3$ receptor and antidepressants within raft-like domains and their antagonistic effects at this ligand-gated ion channel, we investigated the impact of lipid raft integrity for 5-HT$_3$ receptor function and its modulation by antidepressants. Treatment with methyl-β-cyclodextrine (MβCD) markedly reduced membrane cholesterol levels and caused a more diffuse membrane distribution of the lipid raft marker protein flotillin-1 indicating lipid raft impairment. Both amplitude and charge of serotonin evoked cation currents were diminished following cholesterol depletion by either MβCD or simvastatin (Sim), whereas the functional antagonistic properties of the antidepressants desipramine (DMI) and fluoxetine (Fluox) at the 5-HT$_3$ receptor were retained. Although both the 5-HT$_3$ receptor and flotillin-1 were predominantly found in raft-like domains in western blots following sucrose density gradient centrifugation, immunocytochemistry revealed only a coincidental degree of colocalization of these two proteins. These findings and the persistence of the antagonistic effects of DMI and Fluox against 5-HT$_3$ receptors after lipid raft impairment indicate that their modulatory effects are likely mediated through non-raft 5-HT$_3$ receptors, which are not sufficiently detected by means of sucrose density gradient centrifugation. In conclusion, lipid raft integrity appears to be important for 5-HT$_3$ receptor function in general, whereas it is not a prerequisite for the antagonistic properties of antidepressants such as DMI and Fluox at this ligand-gated ion channel.
Neuropsychopharmacology (2010) **35,** 1510–1519; doi:10.1038/npp.2010.20; published online 3 March 2010

Keywords: lipid rafts; antidepressants; 5-HT$_3$ receptor; ligand-gated ion channel; cholesterol; immunocytochemistry

INTRODUCTION

There is increasing evidence that the membrane localization of distinct neurotransmitter receptors within lipid rafts can influence their function by affecting neurotransmitter binding, receptor trafficking, and clustering (Allen *et al*, 2007; Tsui-Pierchala *et al*, 2002). Lipid rafts are specific microdomains within the cell membrane that are enriched in cholesterol and glycosphingolipids (Pike, 2004). They are supposed to be heterogeneous and highly dynamic structures that float within the membrane bilayer (Kusumi and Suzuki, 2005). Lipids and proteins can move in and out of these domains thereby forming distinct clusters, which determine their biophysical properties. In a biochemical sense, lipid rafts are commonly characterized as insoluble by non-ionic detergents upon sucrose density gradient centrifugation at 4°C (Brown and Rose, 1992). However, an

extraction of these microdomains without the use of detergents seems to more closely reflect the physiological situation (Smart *et al*, 1995; Song *et al*, 1996). Thus, different compositions and properties of lipid rafts have been described depending on the preparation procedure (Foster *et al*, 2003; Garner *et al*, 2008; Kim *et al*, 2004; Pike, 2008; Sprenger and Horrevoets, 2007).

Lipid rafts have also been suggested to have a role for the action of antidepressants. It has recently been shown that the G-protein subunit Gsα is more likely shifted to lipid rafts, where it is less likely to couple to adenylyl cyclase, in post mortem brain tissue of patients who had suffered from major depression (Donati *et al*, 2008). Chronic treatment with antidepressants may enhance Gsα signalling through preventing the accumulation of Gsα in lipid rafts (Donati and Rasenick, 2005). Moreover, a variety of antidepressants and antipsychotics accumulate in raft-like domains together with the serotonin type 3 (5-HT$_3$) receptor as detected by sucrose density gradient centrifugation (Eisensamer *et al*, 2005). Indeed, various classes of antidepressants (Breitinger *et al*, 2001; Eisensamer *et al*, 2003; Fan, 1994) and antipsychotics (Rammes *et al*, 2004) have been shown to act as non-competitive antagonists at this neurotransmitter receptor.

The 5-HT$_3$ receptor is a pentameric ligand-gated non-specific cation channel, which functions either as homomeric 5-HT$_{3A}$ or as heteromeric 5-HT$_{3AB}$ receptor (Hannon and Hoyer, 2008; van Hooft and Vijverberg, 2000). However, electrophysiological and immunohistochemical evidence indicates that the majority of native 5-HT$_3$ receptor complexes do not contain the 5-HT$_{3B}$ subunit (Hussy et al, 1994; Reeves and Lummis, 2006; for review see Fletcher and Barnes, 1998). Within the CNS, the 5-HT$_{3A}$ receptor is highly expressed in the area postrema, the caudate nucleus, the hippocampus, and the amygdala (Barnes and Sharp, 1999).

The membrane distribution of the 5-HT$_3$ receptor together with the localization of psychopharmacological drugs within the membrane may thus be crucial for receptor function and its modulation by psychopharmacological drugs. In this study, we therefore investigated as to what extent lipid raft integrity contributes to the functional properties of the 5-HT$_3$ receptor and to the functional antagonistic effects of antidepressants at this ligand-gated ion channel. Lipid raft impairment induced by the cholesterol-depleting agents methyl-β-cyclodextrine (MβCD) or simvastatin (Sim) markedly affected 5-HT$_3$ receptor function. However, the modulation of 5-HT evoked cation currents at the 5-HT$_3$ receptor by the antidepressants desipramine (DMI) and fluoxetine (Fluox) was retained after cholesterol depletion.

MATERIALS AND METHODS

Chemicals and Drugs

Desipramine and Fluox were obtained from Sigma-Aldrich (Deisenhofen, Germany). For stock solutions DMI and Fluox (10 mM) were dissolved in H$_2$O

Cell Cultures

N1E-115 mouse neuroblastoma cells naturally expressing the 5-HT$_{3A}$ receptor were obtained from ATCC LGC Promochem, Wesel, Germany. HEK 293 cells stably expressing the human 5-HT$_{3A}$ receptor were constructed as described previously (Lankiewicz et al, 1998). Cells were cultured in Dulbecco's Modified Eagle's Medium (DMEM; Invitrogen, Karlsruhe, Germany) supplemented with 10% fetal calf serum (FCS; Invitrogen), 1% sodium pyruvate (Invitrogen) and antibiotics (Invitrogen). Cells were re-seeded onto fresh Petri dishes (Josef Peske, Aindlingen-Arnhofen, Germany) twice a week after treatment with 1% trypsin-EDTA (Invitrogen). Cells were cultured at 37°C, 5% CO$_2$, and 95% humidity.

Electrophysiological Recordings

Cells were kept in DMEM without FCS for 12 h before the recordings. Serotonin (5-HT) induced inward Na$^+$-currents were recorded from lifted cells in the whole-cell voltage-clamp configuration under visual control using an inverted microscope (Zeiss, Jena, Germany) as described previously (Rammes et al, 2004). N1E-115 cells were kept in a bath solution containing 162 mM NaCl, 5.3 mM KCl, 0.67 mM Na$_2$HPO$_4$, 0.22 mM KH$_2$PO$_4$, 15 mM HEPES, and 5.6 mM glucose. The bath solution for HEK 293 cells stably expressing the human 5-HT$_{3A}$ receptor consisted of 140 mM NaCl, 2.8 mM KCl, 10 mM HEPES, and 5.6 mM glucose. Both solutions were adjusted to pH 7.2 with NaOH. Patch electrodes were pulled from borosilicate glass (Hilgenberg, Malsfeld, Germany) using a horizontal pipette puller (Zeitz-Instruments, Augsburg, Germany) to yield pipettes with a resistance of 3–6 MΩ. Pipettes were filled with a solution containing 130 mM CsCl, 2 mM MgCl$_2$, 10 mM EGTA, 10 mM HEPES, 2 mM K-ATP, 0.2 mM Tris GTP, 10 mM glucose, pH of 7.2, which was adjusted with CsOH. After the whole-cell configuration was established, the cells were lifted and 30 µM 5-HT for N1E-115 cells or 10 µM 5-HT for HEK 293 cells stably expressing the human 5-HT$_{3A}$ receptor were applied using a fast superfusion device. The respective concentrations of 5-HT were applied since these were used for the determination of the IC$_{50}$ value for the inhibition of the 5-HT response by psychopharmacological drugs in our previous study, which was in the low micromolar range (Rammes et al, 2004). The respective concentrations of DMI and Fluox used to modulate 5-HT$_3$ receptor function during electrophysiological recordings were chosen according to the IC$_{50}$ values of our previous study (Eisensamer et al, 2003) and are achieved in the brain (Baumann et al, 1983; Karson et al, 1993). For control experiments a piezo translator-driven double-barreled application pipette was used to expose the lifted cell either to 5-HT-free or 5-HT-containing solution. A 2 s 5-HT pulse was delivered every 90 s. DMI and Fluox were diluted with bath solution to the desired concentration. Current signals were recorded at a holding potential of −50 mV with an EPC-9 amplifier (Heka, Lamprecht, Germany) and were analyzed using the Heka 8.5 PulseFit and IgorPro v. 5.04B (Wavemetrics, Lake Oswego, OR, USA) software on a Power Macintosh G3 computer. Only results from stable cells showing at least 50% recovery of responses to 5-HT following the removal of drugs entered the final analysis. To compensate for this effect the percentage of antagonism at each concentration was based on both the control and the recovery current by assuming a linear time course for the rundown. The peak amplitude and charge evoked by 5-HT in the absence of cholesterol-depleting compounds or antidepressants was set as 100%. Data were analyzed by the t-test for paired samples.

Sucrose Density Gradient Centrifugation

Two subconfluent Petri dishes (10 cm in diameter) of cells were washed twice in ice-cold PBS (Invitrogen) before resuspension in 800 µl of high-salt HEPES buffer (20 mM HEPES, 5 mM EDTA, 1 M NaCl, pH 7.4) supplemented with a protease-inhibitor cocktail (Sigma-Aldrich). After homogenization and sonication, the suspension was diluted 1:1 with an 80% sucrose stock solution prepared in high-salt HEPES buffer to a final concentration of 40% sucrose. This solution was put to the bottom of a centrifuge tube (Beckman Coulter, Fullerton, CA, USA) and overlaid with 1400 µl of 35% sucrose and finally with 1000 µl of 5% sucrose (both in low-salt HEPES buffer: 20 mM HEPES, 5 mM EDTA, 0.5 M NaCl, pH 7.4). The samples were ultracentrifuged at 40 000 r.p.m. (164 326 × g on average) in a Beckman SW60 rotor for 4 h at 4°C. Thereafter,

10 fractions à 400 μl were taken from the top to the bottom of the gradient.

Western Blotting

Equal volumes of sucrose gradient fractions were adjusted 1:5 with sample buffer (Laemmli: 0.31 M Tris, 25 mM EDTA, 0.5 M DTT, 10% SDS, 500 μl/ml glycerine, 0.33 mg/ml bromophenol blue, pH 6.8) and denatured by heating 5 min at 95°C. SDS/PAGE was performed on 12% gels. After transfer to a nitrocellulose membrane (Whatman, Dassel, Germany) and blocking in TBS-T supplemented with 5% milk powder, blots were probed with specific antibodies to the following antigens: flotillin-1 (mouse monoclonal, BD Biosciences, Heidelberg, Germany, dilution 1:1000), caveolin (rabbit polyclonal, BD Biosciences, dilution 1:5000) and 5-HT$_3$ receptor (rabbit polyclonal, a generous gift from Günter Gisselmann, Lehrstuhl für Zellphysiologie, Ruhr-Universität Bochum, Germany, dilution 1:5000). After incubation with horseradish peroxidase-coupled secondary antibodies, the specific antibody binding was visualized by ECL chemiluminescence (Amersham Biosciences, Freiburg, Germany).

Immunocytochemistry

Cells were cultured on poly-L-lysine coated 4-chamber culture slides (BD Biosciences). Cells were fixed in 4% paraformaldehyde for 10 min at room temperature. Afterwards, permeabilization was carried out with 0.2% Triton X-100 in PBS for 5 min. Blocking in PBS supplemented with 5% BSA for 2 h was followed by incubation with primary antibodies overnight at 4°C (anti-5-HT$_3$ receptor rabbit polyclonal, Calbiochem, Gibbstown, NJ, USA, dilution 1:25; flotillin-1 mouse monoclonal, BD Biosciences, dilution 1:100) in PBS supplemented with 5% BSA and 0.1% Triton X-100. Secondary antibody incubation (Cy3 anti-mouse, Dianova, Hamburg, Germany and biotin-SP-conjugated anti-rabbit, Dianova) in PBS supplemented with 5% BSA and 0.1% Triton X-100 was performed for 1 h at room temperature and followed by tertiary antibody treatment (avidin-conjugated Alexa Flour 488, Molecular Probes, Eugene, OR, USA) and 4′,6-diamidino-2-phenylindole dihydrochloride (DAPI, Dianova) for one further hour at room temperature (in PBS supplemented with 5% BSA and 0.1% Triton X-100). Culture slides were examined using confocal laser microscopy (Olympus FV 1000D, Hamburg, Germany). Quantitative colocalization data were analyzed by one-way ANOVA.

Cholesterol Depletion

For cholesterol depletion cells were either treated with MβCD (Sigma-Aldrich) or Sim (Sigma-Aldrich). When MβCD was used, cells were incubated with 0.5 mM up to 7.5 mM for 12 h at 37°C in serum-free DMEM. To maintain cell viability and to retain the possibility to obtain functional data by whole-cell voltage-clamp recordings we chose a rather low concentration (0.5 mM) coupled with a prolonged application time (12 h), because serotonin evoked cation currents could not be recorded any more after treatment of cells with higher concentrations of MβCD.

For Sim-induced cholesterol depletion, cells were kept in serum-free DMEM for 12 h before Sim was added at a concentration of 0.5 μM for 24 h at 37°C.

Preparation of Cell Membranes for Cholesterol/Protein Measurements

For cholesterol or protein quantification, one Petri dish (10 cm in diameter) of cells was first washed twice in ice-cold PBS before resuspension in 300 μl of high-salt HEPES buffer supplemented with protease-inhibitor cocktail before homogenization and sonication. The suspension was then centrifuged for 10 min at 1000 g at 4°C. The supernatant was again centrifuged at 8000 g for further 10 min at 4°C. This second supernatant was assayed for cholesterol and protein concentrations.

Cholesterol and Protein Assay

Cell cholesterol concentrations were determined colorimetrically with a commercial assay kit (Boehringer, Mannheim, Germany) according to the manufacturer's recommendations. Cell protein concentrations were determined by a modified method of Lowry et al. (1951). Data were analyzed using Student's t-test.

RESULTS

Effects of Cholesterol Depletion on 5-HT$_3$ Receptor Function

Because withdrawal of cholesterol from cell membranes by means of MβCD is a commonly used approach for lipid raft disruption, we investigated whether cholesterol depletion by MβCD affects 5-HT$_3$ receptor function using whole-cell voltage-clamp recordings. Treatment of N1-E115 cells kept in DMEM without fetal calf serum (FCS) with 0.5 mM MβCD for 12 h markedly reduced the peak amplitude and increased onset, desensitization and deactivation kinetics of serotonin evoked cation currents under cholesterol-depleting conditions, whereas charge was less affected (Figure 1a, Table 1). 0.5 mM was the maximum dose of MβCD which still allowed whole-cell voltage-clamp recordings (data not shown).

To verify lipid raft impairment under these experimental conditions we quantified cholesterol levels in membranes of N1E-115 cells, which were reduced to 43.9% by treatment with MβCD (Figure 2a). Moreover, immunocytochemistry revealed a more diffuse distribution of the lipid raft marker protein flotillin-1 upon cholesterol depletion by MβCD (Figure 2b). The apparent increase in signal intensity of flotillin-1 following MβCD treatment in immunocytochemistry was not related to an altered expression of this protein as shown by western blot analysis (Figure 2c). Apparently, treatment with MβCD under these experimental conditions affects both lipid raft integrity and 5-HT$_3$ receptor function.

When cells were kept in DMEM supplemented with 10% FCS, MβCD-induced cholesterol depletion was prevented due to the presence of cholesterol in FCS (data not shown). Nevertheless, MβCD treatment reduced the amplitude, although to a smaller degree than under cholesterol-depleting conditions, and, in contrast to cholesterol

depleting conditions, accelerated receptor desensitization and deactivation (Figure 1b, Table 1).

As an alternative approach for cholesterol depletion we used the hydroxyl-methylglutaryl-coenzyme A reductase inhibitor Sim, which inhibits endogenous cholesterol synthesis. Treatment with $0.5\,\mu M$ Sim for $24\,h$ reduced serotonin-evoked cation currents in a similar way as did cholesterol depletion by $M\beta CD$ (Table 1).
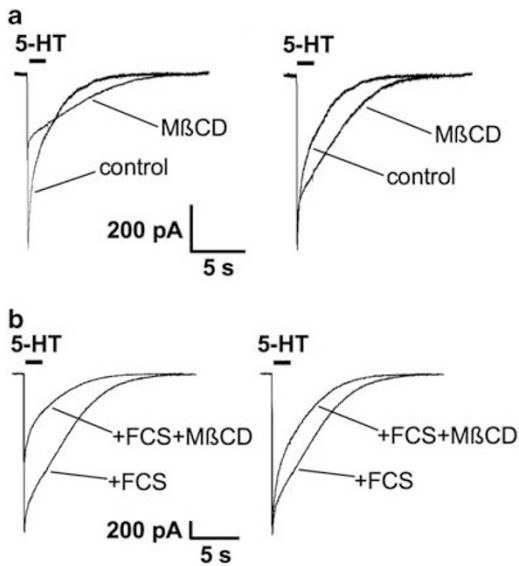

Figure I Treatment with $M\beta CD$ decreases serotonin-evoked cation currents in N1E-115 cells. (a) Effect of $M\beta CD$ under cholesterol-depleting conditions. Cation currents were recorded in a whole-cell voltage-clamp configuration. $30\,\mu M$ 5-HT was applied for $2\,s$. The left panel shows representative recordings of an untreated cell (control; without FCS) and of a cell pretreated with $0.5\,mM$ $M\beta CD$ for $12\,h$ ($M\beta CD$). The left panel shows currents of a representative experiment, the right panel shows the same recording normalized to control. (b) Effect of $M\beta CD$ in the presence of FCS avoiding cholesterol depletion. Cation currents were recorded in a whole-cell voltage-clamp configuration. $30\,\mu M$ 5-HT was applied for $2\,s$. The left panel shows representative recordings of an untreated cell in the presence of FCS (+FCS) and of a cell pretreated with $0.5\,mM$ $M\beta CD$ for $12\,h$ (+FCS +$M\beta CD$). Cells were kept in DMEM with FCS for $12\,h$ both during control and during $M\beta CD$ incubation before the recordings. The left panel shows currents of a representative experiment, the right panel shows the same recording normalized to the untreated cell +FCS.

Effects of Cholesterol Depletion on the Antagonistic Effects of Antidepressants at the 5-HT$_3$ Receptor

To address the question of whether impairment of lipid raft integrity also affects the modulation of the 5-HT$_3$ receptor by antidepressants we studied the impact of cholesterol depletion on the functional antagonistic effects of DMI and Fluox at this ligand-gated ion channel.

The tricyclic antidepressant DMI reduced the peak amplitude and charge of serotonin-evoked cation currents and accelerated the decay in N1E-115 cells as reported previously (Eisensamer et al, 2003) (Figures 3a and d, Table 2). Although treatment with $0.5\,mM$ $M\beta CD$ for $12\,h$ markedly diminished 5-HT$_3$ receptor currents, the DMI-induced inhibition and kinetic changes were still retained following cholesterol depletion by $M\beta CD$ (Figures 3b and d, Table 2). Also after treatment with $0.5\,\mu M$ Sim for $24\,h$, DMI still reduced serotonin-evoked cation currents and accelerated receptor kinetics in N1E-115 cells with similar potency as after incubation with $M\beta CD$ (Figures 3c and d, Table 2). Moreover, the antagonistic effect of DMI on serotonin-evoked cation currents was maintained following $M\beta CD$ treatment also in HEK 293 cells stably expressing the human 5-HT$_{3A}$ receptor (data not shown). Concerning other antidepressant compounds, comparable findings were obtained when the selective serotonin reuptake inhibitor Fluox was applied. The antagonistic potency against the peak amplitude and charge and the Fluox-induced acceleration of receptor desensitization could be observed both in control experiments (Figures 4a and c, Table 3) and under conditions of $M\beta CD$-induced cholesterol depletion (Figures 4b and c, Table 3).

Differential Distribution of the 5-HT$_3$ Receptor and Flotillin-1 in Sucrose Density Gradients and in Immunocytochemistry

In view of the persistent antagonistic effects of antidepressants at the 5-HT$_3$ receptor even under cholesterol depleted conditions we investigated as to what extent cholesterol depletion leads to lipid raft disruption. Although treatment with $0.5\,mM$ $M\beta CD$ for $12\,h$ markedly reduced membrane cholesterol levels and affected flotillin-1 distribution in immunocytochemistry, flotillin-1 still remained in the low

Table I Effect of $M\beta CD$ on Serotonin-Evoked Cation Currents of N1E-115 Cells

	Control	+$M\beta CD$	+Sim	+FCS	+FCS+$M\beta CD$
τ_{on} (ms)	26.6 ± 4.4	80.7 ± 17.5 (303.4%)[a]	26.0 ± 3.8 (97.7%)[a]	19.8 ± 1.7	21.8 ± 2.4 (110.1%)[b]
τ_{des} (ms)	546.0 ± 30.0	1429.4 ± 196.4 (261.8%)[a]	1215.8 ± 166.1 (222.7%)[a]	1337.8 ± 216.1	876.1 ± 92.5 (65.5%)[b]
τ_{off} (ms)	1938.0 ± 65.3	4010.2 ± 262.1 (206.9%)[a]	3480.2 ± 281.2 (179.6%)[a]	3715.5 ± 150.5	3091.9 ± 172.6 (83.2%)[b]
peak (pA)	-714.7 ± 60.1	-242.9 ± 51.0 (34.0%)[a]	-363.1 ± 111.3 (50.8%)[a]	-1845.3 ± 127.4	-1262.5 ± 116.7 (68.4%)[b]
charge (pC)	-1695 ± 502.7	-1395 ± 371.8 (82.3%)[a]	-1229 ± 500.8 (72.5%)[a]	-8295 ± 808.2	-3123 ± 623.9 (37.6%)[b]

Time constants (τ) of onset (τ_{on}), desensitization (τ_{des}) and offset (τ_{off}), peak amplitudes and charges of 5-HT-evoked cation currents of N1E-115 cells under the following conditions: control: cells were kept in DMEM without FCS for $12\,h$; +$M\beta CD$: cells were treated with $M\beta CD$ $0.5\,mM$ for $12\,h$ in DMEM without FCS; +Sim: cells were treated with Sim $0.5\,\mu M$ for $24\,h$ in DMEM without FCS; +FCS: cells were kept in DMEM supplemented with 10% FCS; +FCS+$M\beta CD$: cells were kept in DMEM supplemented with 10% FCS and were treated with $M\beta CD$ $0.5\,mM$ for $12\,h$. Results are shown as the mean $\pm$ SEM of 10 independent experiments for control, +$M\beta CD$, +FCS, +FCS+$M\beta CD$, respectively, with the exception of +Sim ($n = 6$).
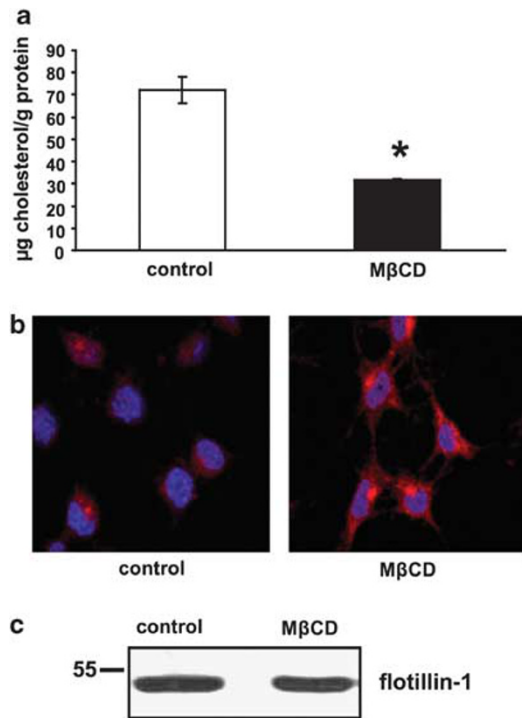[a]Percent of control.
[b]Percent of+FCS.

sensitivity to cholesterol depletion cannot be completely excluded.

To rule out potential direct pharmacological effects of MβCD on 5-HT evoked cation currents independent from cholesterol depletion N1E-115 cells were kept in medium supplemented with 10% FCS before and during MβCD treatment thereby preventing cholesterol depletion. The effects of MβCD on 5-HT-evoked cation currents under these experimental conditions were far less pronounced and clearly distinguishable from those of cholesterol depletion.

As another approach to show lipid raft impairment under our experimental conditions we investigated the membrane distribution of the lipid raft marker protein flotillin-1 by means of immunocytochemistry. Treatment with MβCD caused a more diffuse membrane distribution of flotillin-1 along with an apparent signal enhancement of flotillin-1, which was not due to a higher expression of the protein but

might reflect an increased availability of the flotillin-1 epitope for detection by the respective antibody. This phenomenon of increased immunoreactivity of lipid raft-associated proteins following MβCD treatment has already been observed previously. For example, the enhancement of cannabinoid 1 (CB1) receptor immunoreactivity expressed in rat C6 glioma cells following MβCD treatment has also been suggested to be dependent on an increased accessibility of protein binding sites to specific antibodies (Bari et al, 2008). Thus, cholesterol depletion under these experimental conditions affects lipid raft integrity, although a complete lipid raft disruption remains questionable. We therefore titrated the concentration of MβCD necessary to shift flotillin-1 to the HBD fractions of sucrose density gradients and we found that at least 15-fold higher concentration of MβCD was required, which does not allow whole-cell voltage-clamp recordings anymore, due to severe cell damage. These results suggest that impairment of lipid rafts by cholesterol depletion is not necessarily detected by
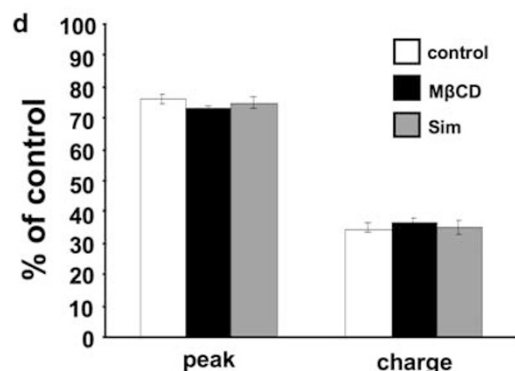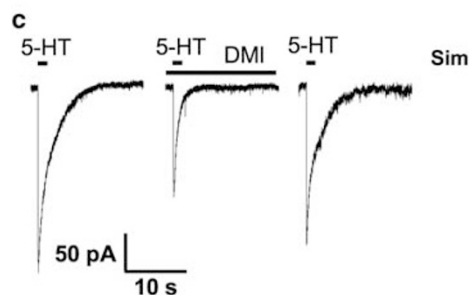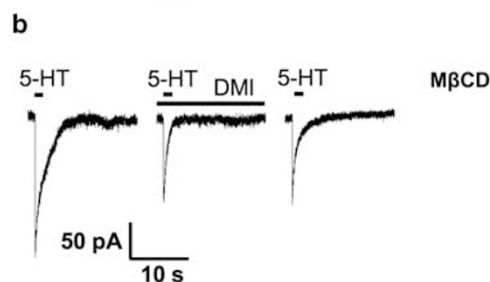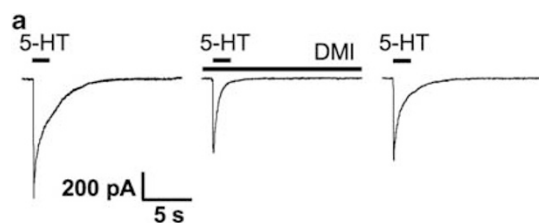

Table 2 Effect of MβCD and Sim on the Modulation of 5-HT$_3$ Receptor Kinetics by DMI

	DMI	DMI+MβCD	DMI+Sim
τ_{on} %	162.2 ± 1.7	156.5 ± 9.0	160.7 ± 11.0
τ_{des} %	77.9 ± 2.1	79.1 ± 2.8	78.7 ± 16.5
τ_{off} %	89.9 ± 18.1	60.9 ± 16.1	54.9 ± 8.1

Time constants (τ) of onset (τ_{on}), desensitization (τ_{des}) and offset (τ_{off}) of 5-HT evoked cation currents of N1E-115 cells under the following conditions: DMI: application of DMI, DMI+MβCD: application of DMI to cells pretreated with MβCD 0.5 mM, DMI+Sim: application of DMI to cells pretreated with Sim 0.5 μM. Results are shown as mean ± SEM % of control (see Figure 3d) of six independent experiments.

Figure 3 The modulation of serotonin evoked currents by DMI is retained after MβCD or Sim treatment of N1E-115 cells. (a) Antagonistic effect of DMI at the 5-HT$_3$ receptor. Cation currents were recorded in a whole-cell voltage-clamp configuration. 30 μM 5-HT were applied for 2 s in the absence or presence of 1 μM DMI. The upper bars indicate the presence of 5-HT, the lower bar indicates the presence of DMI. Representative recordings before and after application of DMI and subsequent washout are shown. (b) Antagonistic effect of DMI after MβCD treatment. Cation currents were recorded in a whole-cell voltage-clamp configuration. 30 μM 5-HT were applied for 2 s in the absence or presence of 1 μM DMI. The upper bars indicate the presence of 5-HT, the lower bar indicates the presence of DMI. Representative recordings before and after application of DMI and subsequent washout are shown. Cells were treated with 0.5 mM MβCD for 12 h before the recordings. (c) Antagonistic effect of DMI after Sim treatment. Cation currents were recorded in a whole-cell voltage-clamp configuration. 30 μM 5-HT were applied for 2 s in the absence or presence of 1 μM DMI. The upper bars indicate the presence of 5-HT, the lower bar indicates the presence of DMI. Representative recordings before and after application of DMI and subsequent washout are shown. Cells were treated with 0.5 μM Sim for 24 h before the recordings. (d) Peak amplitude and charge of controls (white bars) and after pretreatment with 0.5 mM MβCD for 12 h (black bars) or 0.5 μM Sim for 24 h (grey bars) in the presence of DMI of six independent experiments in relation to values in the absence of DMI, which are set as 100%. Data are shown as mean ± SEM % of control. DMI reduces peak amplitude and charge to a similar degree in all three experimental conditions.
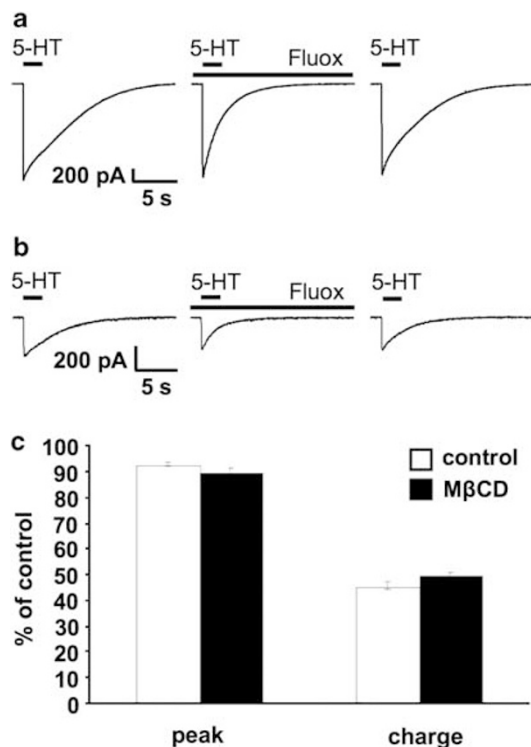
Figure 4 The modulation of serotonin evoked currents by Fluox is retained after MβCD treatment of N1E-115 cells. (a) Antagonistic effect of Fluox at the 5-HT$_3$ receptor. Cation currents were recorded in a whole-cell voltage-clamp configuration. 30 μM 5-HT were applied for 2 s in the absence or presence of 3 μM Fluox. The upper bars indicate the presence of 5-HT, the lower bar indicates the presence of Fluox. Representative recordings before and after application of Fluox and subsequent washout are shown. (b) Antagonistic effect of Fluox after MβCD treatment. Cation currents were recorded in a whole-cell voltage-clamp configuration. 30 μM 5-HT was applied for 2 s in the absence or presence of 3 μM Fluox. The upper bars indicate the presence of 5-HT, the lower bar indicates the presence of Fluox. Representative recordings before and after application of Fluox and subsequent washout are shown. Cells were treated with 0.5 mM MβCD for 12 h before the recordings. (c) Peak amplitude and charge of controls (white bars) and after pretreatment with 0.5 mM MβCD for 12 h (black bars) in the presence of Fluox of six independent experiments in relation to values in the absence of Fluox, which are set as 100%. Data are shown as mean ± SEM % of control. Fluox reduces peak amplitude and charge to a similar degree in both experimental conditions.

Table 3 Effect of MβCD on the Modulation of 5-HT$_3$ Receptor Kinetics by Fluox

	Fluox	Fluox+MβCD
τ_{on} %	98.1 ± 5.1	100.6 ± 3.9
τ_{des} %	96.1 ± 12.9	84.6 ± 1.3
τ_{off} %	47.3 ± 1.2	54.0 ± 4.2

Time constants (τ) of onset (τ$_{on}$), desensitization (τ$_{des}$) and offset (τ$_{off}$) of 5-HT evoked cation currents of N1E-115 cells under the following conditions: Fluox: application of Fluox, Fluox+MβCD: application of Fluox to cells pretreated with MβCD 0.5 mM. Results are shown as mean ± SEM % of control (see Figure 4c) of six independent experiments.

sucrose density gradients under experimental conditions needed to perform functional investigations such as electrophysiological recordings.
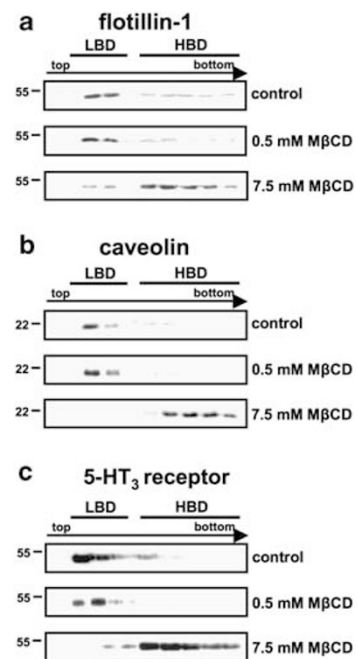
Figure 5 Treatment with high concentrations of MβCD shifts flotillin-1, caveolin, and the 5-HT$_3$ receptor to the high buoyant density fractions (HBD) in sucrose gradients of HEK 293 cells stably expressing the human 5-HT$_{3A}$ receptor. Living cells were treated with MβCD for 12 h at different concentrations (0.5 and 7.5 mM); one proportion of the cells remained untreated (control). Cells were then homogenized, sonicated in high-salt HEPES buffer, and fractionated by sucrose gradient density centrifugation. Thereafter, 10 fractions were collected from the top to the bottom of the gradient and analyzed by SDS-PAGE. Replicate gels were immunoblotted with antibodies against flotillin-1 (a), caveolin (b) and the 5-HT$_3$ receptor (c). The blots shown are representative gradients out of three independent experiments. LBD: low buoyant density fractions; HBD: high buoyant density fractions.

With regard to 5-HT$_3$ receptor function, there was a significant reduction in peak amplitude and charge of serotonin evoked cation currents after depletion of cholesterol with 0.5 mM MβCD in spite of a prolongation of receptor desensitization and deactivation. Simvastatin, through its ability to inhibit the synthesis of endogenous cholesterol, is considered as an alternative approach for lipid raft impairment (Ponce et al, 2008; Sjögren et al, 2006) and exerted similar effects on serotonin evoked cation currents. The pronounced reduction of the peak amplitude after cholesterol depletion by MβCD was indeed due to cholesterol depletion, as acute application of 0.5 mM MβCD did not affect the peak amplitude but prolonged the decay for deactivation kinetics thus increasing the charge (data not shown). These findings support the hypothesis that the function of the 5-HT$_3$ receptor largely depends on the cholesterol content of the membrane, even if there is no complete raft disruption under cholesterol-depleted conditions. Nevertheless, lipid raft integrity appears to be important for physiological receptor function in view of the localization of this ligand-gated ion channel in raft-like domains in sucrose density gradients (Eisensamer et al, 2005).

Since certain antidepressants are enriched in LBD fractions of sucrose density gradients and their concentrations within LBD fractions are related to their antagonistic

potency against 5-HT$_3$ receptors (Eisensamer et al, 2005), it might be hypothesized that lipid raft integrity is a major determinant for the allosteric modulation of the 5-HT$_3$ receptor channel by antidepressants. Unexpectedly, the antagonistic potency of antidepressants against serotonin evoked cation currents was retained following cholesterol depletion by either MβCD or Sim in spite of a pronounced overall reduction of serotonin-evoked currents. This is further underlined by the observation that both DMI and Fluox, which are enriched in LBD fractions of sucrose density gradients (Eisensamer et al, 2005), accelerated receptor desensitization even under conditions of cholesterol depletion. These findings challenge the hypothesis that 5-HT$_3$ receptor integration within lipid rafts is an indispensable prerequisite for the non-competitive antagonistic effects of antidepressants or antipsychotics at the 5-HT$_3$ receptor (Eisensamer et al, 2003; Rammes et al, 2004) and

that these effects are predominantly conferred through an interaction with 5-HT$_3$ receptors within raft-like domains.

In view of this apparent discrepancy we reinvestigated the colocalization of the 5-HT$_3$ receptor with the lipid raft marker protein flotillin-1 both by means of western blots of sucrose density gradient fractions and by immunocytochemistry. We could replicate our previous findings that both the 5-HT$_3$ receptor protein and flotillin-1 are predominantly found in the LBD fractions of sucrose density gradients (Eisensamer et al, 2005), which is compatible with a localization within raft-like domains. Treatment with high concentrations of MβCD shifted both the 5-HT$_3$ receptor protein and flotillin-1 to the HBD fractions, which was not observed with 0.5 mM MβCD in spite of an effect of this concentration on membrane cholesterol content and redistribution of flotillin-1 in immunocytochemistry. In contrast to the findings obtained with sucrose density gradients, immunocytochemistry revealed only a coincidental degree of colocalization of the 5-HT$_3$ receptor and flotillin-1 in the absence of cholesterol-depleting agents, which suggests that only a minor proportion of 5-HT$_3$ receptors is constantly present in lipid rafts.

Because lipid rafts are believed to be highly dynamic structures, the determination of whether a distinct protein is raft associated or not is a technical challenge, which largely relies on the respective technique employed. Several studies report a lower rate of colocalization of 'raft-candidate proteins' and even an underestimation of raft association by means of immunocytochemistry when compared with biochemical methods such as sucrose density gradient centrifugation (for review see Kusumi and Suzuki, 2005), which is in line with our results. For example, the membrane localization of glycophosphatidylinositol-anchored proteins such as the folate receptor
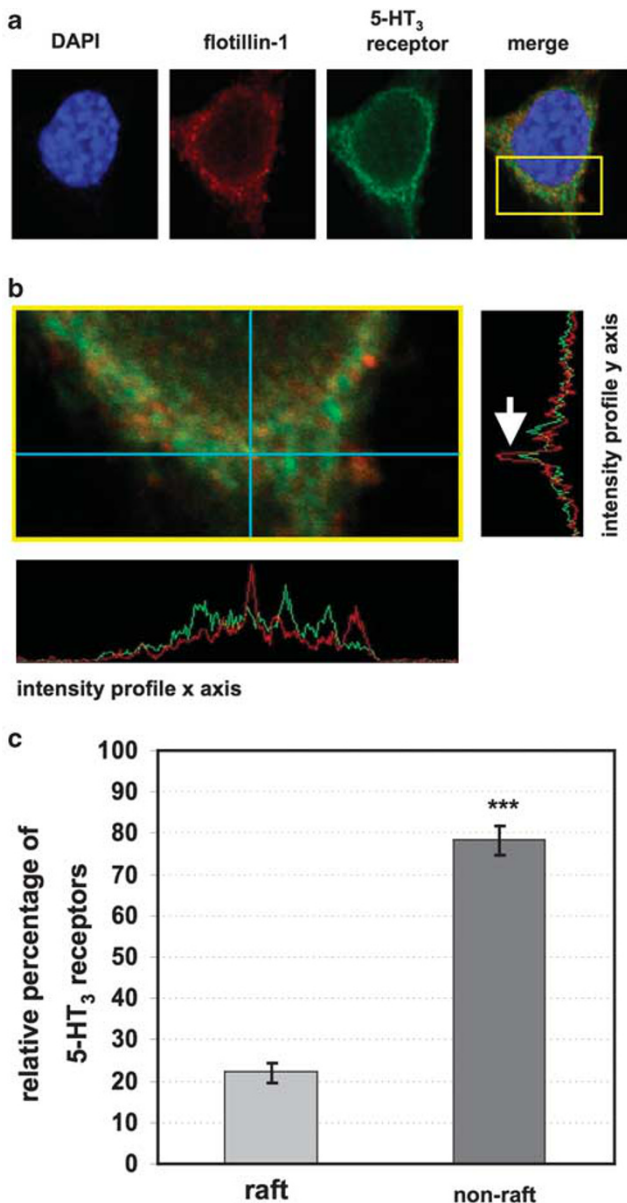

Figure 6 Low degree of colocalization of the 5-HT$_3$ receptor with the lipid raft marker protein flotillin-1 in N1E-115 cells using immunofluorescence. (a) Cells were fixed, permeabilized, and immunostained with an antibody against flotillin-1 (red spots) and against the 5-HT$_3$ receptor (green spots). Cell nuclei were stained in blue with DAPI. Immunofluorescence was recorded at a 60-fold magnification and a 6-fold zoom. Colocalization of flotillin-1 and the 5-HT$_3$ receptor is indicated by the superposition of red and green fluorescence in the form of yellow spots (merge). Representative images out of five independent experiments are shown. (b) Magnification of the merged images from the yellow box in (a) without DAPI. Intensity profiles along the blue lines of the red channel (flotillin-1) and the green channel (5-HT$_3$ receptor) show only a low degree of colocalization of flotillin-1 and the 5-HT$_3$ receptor (white arrow). (c) The proportion of double-labeled spots within one cell (flotillin-1 labeled (flotillin-1$^+$) and 5-HT$_3$ receptor labeled (5-HT$_3^+$) was quantified in relation to the total number of flotillin-1$^+$ spots to assess the relative percentage of raft-associated 5-HT$_3$ receptors (raft). This was compared with the proportion of 5-HT$_3$ receptor$^+$/flotillin-1 non-labeled (flotillin-1$^-$) spots in relation to total 5-HT$_3$ receptor$^+$ spots to quantify the relative percentage of non-raft-associated 5-HT$_3$ receptors (non-raft). The relative percentage of raft-5-HT$_3$ receptors was significantly lower (21.9 $\pm$ 2.3%) in comparison with that of non-raft-5-HT$_3$ receptors (78.2 $\pm$ 3.6%) as indicated by one-way ANOVA analysis of the results from five independent experiments (F$_{(1)}$ = 161.96; ***$p \leqslant 0.001$). There was no difference in immunofluorescence patterns between cells kept in DMEM supplemented with 10% FCS compared with cells kept in serum-free DMEM for 12 h before immunocytochemistry (data not shown).

seems to be related to multimerization processes, which, in turn, were influenced by the chemical fixation procedure in immunocytochemistry (Mayor *et al*, 1994). As another example, also the sodium-taurocholate cotransporting polypeptide in mouse liver yielded divergent results in immunocytochemical colocalization with caveolin-1 and western blots of sucrose density gradient fractions (Molina *et al*, 2008).

Possible explanations for these discrepancies between immunofluorescence colocalization studies and biochemical techniques are the liability of the respective results to subtle variations in experimental protocols and the observation that transient and dynamic interactions with lipid rafts are often missed (Kusumi and Suzuki, 2005). As such, detection of raft or non-raft association of proteins in a dynamic system may be preferentially detected by the respective method employed and, therefore, a combination of different methodological approaches as applied in our study gives a more realistic picture than just a single method. Our observations that the functional antagonistic effects of antidepressants at the 5-HT$_3$ receptor are retained in spite of cholesterol depletion together with the results from immunocytochemistry argue against the hypothesis that receptor integration within lipid rafts is the major determinant for these modulatory effects.

In conclusion, 5-HT$_3$ receptors appear to be raft and non-raft associated within a dynamic system. This differential membrane localization may have a role for receptor function. However, lipid raft integrity is not a prerequisite for the allosteric modulation of this ligand-gated ion channel by antidepressants.

DISCLOSURE

Each author certifies that he or she has no commercial associations that might pose a conflict of interest in connection with the submitted article.

REFERENCES

Allen JA, Halverson-Tamboli RA, Rasenick MM (2007). Lipid raft microdomains and neurotransmitter signalling. *Nat Rev Neurosci* **8**: 128–140.

Bari M, Oddi S, De Simone C, Spagnolo P, Gasperi V, Battista N *et al* (2008). Type-1 cannabinoid receptors colocalize with caveolin-1 in neuronal cells. *Neuropharmacology* **54**: 45–50.

Barnes NM, Sharp T (1999). A review of central 5-HT receptors and their function. *Neuropharmacology* **38**: 1083–1152.

Barrantes FJ (2007). Cholesterol effects on nicotinic acetylcholine receptor. *J Neurochem* **103**(Suppl 1): 72–80.

Baumann P, Gaillard JM, Perey M, Justafre JC, Le P (1983). Relationships between brain concentrations of desipramine and paradoxical sleep inhibition in the rat. *J Neural Transm* **56**: 105–116.

Breitinger HG, Geetha N, Hess GP (2001). Inhibition of the serotonin 5-HT$_3$ receptor by nicotine, cocaine, and fluoxetine investigated by rapid chemical kinetic techniques. *Biochemistry* **40**: 8419–8429.

Brown DA, Rose JK (1992). Sorting of GPI-anchored proteins to glycolipid-enriched membrane subdomains during transport to the apical cell surface. *Cell* **68**: 533–544.

Christian AE, Haynes MP, Phillips MC, Rothblat GH (1997). Use of cyclodextrins for manipulating cellular cholesterol content. *J Lipid Res* **38**: 2264–2272.

Donati RJ, Dwivedi Y, Roberts RC, Conley RR, Pandey GN, Rasenick MM (2008). Postmortem brain tissue of depressed suicides reveals increased Gs alpha localization in lipid raft domains where it is less likely to activate adenylyl cyclase. *J Neurosci* **28**: 3042–3050.

Donati RJ, Rasenick MM (2005). Chronic antidepressant treatment prevents accumulation of gsalpha in cholesterol-rich, cytoskeletal-associated, plasma membrane domains (lipid rafts). *Neuropsychopharmacology* **30**: 1238–1245.

Eisensamer B, Rammes G, Gimpl G, Shapa M, Ferrari U, Hapfelmeier G *et al* (2003). Antidepressants are functional antagonists at the serotonin type 3 (5-HT$_3$) receptor. *Mol Psychiatry* **8**: 994–1007.

Eisensamer B, Uhr M, Meyr S, Gimpl G, Deiml T, Rammes G *et al* (2005). Antidepressants and antipsychotic drugs colocalize with 5-HT$_3$ receptors in raft-like domains. *J Neurosci* **25**: 0198–10206.

Fan P (1994). Inhibition of a 5-HT$_3$ receptor-mediated current by the selective serotonin uptake inhibitor, fluoxetine. *Neurosci Lett* **173**: 210–212.

Fletcher S, Barnes NM (1998). Desperately seeking subunits: are native 5-HT$_3$ receptors really homomeric complexes? *Trends Pharmacol Sci* **19**: 212–215.

Foster LJ, De Hoog CL, Mann M (2003). Unbiased quantitative proteomics of lipid rafts reveals high specifity for signaling factors. *Proc Natl Acad Sci USA* **100**: 5813–5818.

Garner AE, Smith DA, Hooper NM (2008). Visualization of detergent solubilization of membranes: implications for the isolation of rafts. *Biophys J* **94**: 1326–1340.

Hannon J, Hoyer D (2008). Molecular biology of 5-HT receptors. *Behav Brain Res* **195**: 198–213.

Hering H, Lin CC, Sheng M (2003). Lipid rafts in the maintenance of synapses, dendritic spines, and surface AMPA receptor stability. *J Neurosci* **23**: 3262–3271.

Hussy N, Lukas W, Jones KA (1994). Functional properties of a cloned 5-hydroxytryptamine ionotropic receptor subunit: comparison with native mouse receptors. *J Physiol* **481**(Part 2): 311–323.

Karson CN, Newton JE, Livingston R, Jolly JB, Cooper TB, Springg J *et al* (1993). Human brain fluoxetine concentrations. *J Neuropsychiatry Clin Neurosci* **5**: 322–329.

Kilsdonk EP, Yancey PG, Stoudt GW, Bangerter FW, Johnson WJ, Phillips MC *et al* (1995). Cellular cholesterol efflux mediated by cyclodextrins. *J Biol Chem* **270**: 17250–17256.

Kim KB, Kim SI, Choo HJ, Kim JH, Ko YG (2004). Two-dimensional electrophoretic analysis reveals that lipid rafts are intact at physiological temperature. *Proteomics* **4**: 3527–3535.

Kusumi A, Suzuki K (2005). Toward understanding the dynamics of membrane-raft-based molecular interactions. *Biochim Biophys Acta* **1746**: 234–251.

Lankiewicz S, Lobitz N, Wetzel CH, Rupprecht R, Gisselmann G, Hatt H (1998). Molecular cloning, functional expression, and pharmacological characterization of 5-hydroxytryptamine 3 receptor cDNA and its splice variants from guinea pig. *Mol Pharmacol* **53**: 202–212.

Liu M, Huang W, Wu D, Priestley JV (2006). TRPV1, but not P2X, requires cholesterol for its function and membrane expression in rat nociceptors. *Eur J Neurosci* **24**: 1–6.

London E (2005). How principles of domain formation in model membranes may explain ambiguities concerning lipid raft formation in cells. *Biochim Biophys Acta* **1746**: 203–220.

Lowry OH, Rosebrough NJ, Farr AL, Randall RJ (1951). Protein measurement with the Folin phenol reagent. *J Biol Chem* **193**: 265–275.

Mayor S, Rothberg KG, Maxfield FR (1994). Sequestration of GPI-anchored proteins in caveolae triggered by cross-linking. *Science* **264**: 1948–1951.

Molina H, Azocar L, Ananthanarayanan M, Arrese M, Miquel JF (2008). Localization of the sodium-taurocholate cotransporting polypeptide in membrane rafts and modulation of its activity by cholesterol *in vitro*. *Biochim Biophys Acta* **1778**: 1283–1291.

Pike LJ (2004). Lipid rafts: heterogeneity on the high seas. *Biochem J* **378**: 281–292.

Pike LJ (2008). The challenge of lipid rafts. *J Lipid Res* **50**: S323–S328.

Ponce J, de la Ossa NP, Hurtado O, Millan M, Arenillas JF, Davalos A *et al* (2008). Simvastatin reduces the association of NMDA receptors to lipid rafts: a cholesterol-mediated effect in neuroprotection. *Stroke* **39**: 1269–1275.

Pucadyil TJ, Chattopadhyay A (2004). Cholesterol modulates ligand binding and G-protein coupling to serotonin(1A) receptors from bovine hippocampus. *Biochim Biophys Acta* **1663**: 188–200.

Rammes G, Eisensamer B, Ferrari U, Shapa M, Gimpl G, Gilling K *et al* (2004). Antipsychotic drugs antagonize human serotonin type 3 receptor currents in a noncompetitive manner. *Mol Psychiatry* **9**: 846–858.

Reeves DC, Lummis SC (2006). Detection of human and rodent 5-HT$_{3B}$ receptor subunits by anti-peptide polyclonal antibodies. *BMC Neurosci* **7**: 27.

Sjögren B, Hamblin MW, Svenningsson P (2006). Cholesterol depletion reduces serotonin binding and signaling via human 5-HT$_{7a}$ receptors. *Eur J Pharmacol* **552**: 1–10.

Smart EJ, Ying YS, Mineo C, Anderson RG (1995). A detergent-free method for purifying caveolae membrane from tissue culture cells. *Proc Natl Acad Sci USA* **92**: 10104–10108.

Song KS, Li Shengwen, Okamato T, Quilliam LA, Sargiacomo M, Lisanti MP (1996). Co-purification and direct interaction of ras with caveolin, an integral membrane protein of caveolae microdomains. Detergent-free purification of caveolae micro-domains. *J Biol Chem* **271**: 9690–9697.

Sooksawate T, Simmonds MA (2001a). Influence of membrane cholesterol on modulation of the GABA(A) receptor by neuroactive steroids and other potentiators. *Br J Pharmacol* **134**: 1301–1311.

Sooksawate T, Simmonds MA (2001b). Effects of membrane cholesterol on the sensitivity of the GABA(A) receptor to GABA in acutely dissociated rat hippocampal neurones. *Neuropharmacol* **40**: 178–184.

Sprenger RR, Horrevoets AJ (2007). The ins and outs of lipid domain proteomics. *Proteomics* **7**: 2895–2903.

Tsui-Pierchala BA, Encinas M, Milbrandt J, Johnson Jr EM (2002). Lipid rafts in neuronal signaling and function. *Trends Neurosci* **25**: 412–417.

van Hooft JA, Vijverberg HP (2000). 5-HT(3) receptors and neurotransmitter release in the CNS: a nerve ending story? *Trends Neurosci* **23**: 605–610.

Yancey PG, Rodrigueza WV, Kilsdonk EP, Stoudt GW, Johnson WJ, Phillips MC *et al* (1996). Cellular cholesterol efflux mediated by cyclodextrins. Demonstration of kinetic pools and mechanism of efflux. *J Biol Chem* **271**: 16026–16034.